Published in final edited form as:
Calcif Tissue Int. 2010 June ; 86(6): 470–483. doi:10.1007/s00223-010-9359-y.

Age-Related Changes in Bone Structure and Strength in Female and Male BALB/c Mice

Mark D. Willingham[1,2], **Michael D. Brodt**[1], **Kristen L. Lee**[1,2], **Abby L. Stephens**[1,2], **Jiaxin Ye**[2], and **Matthew J. Silva**[1,2]

[1]Department of Orthopaedic Surgery, Washington University, Saint Louis, Missouri, USA

[2]Department of Biomedical Engineering, Washington University, Saint Louis, Missouri, USA

Abstract

Mice may be useful for studies of skeletal aging, but there are limited data on changes in bone structure and strength over their lifespan. We obtained bones from female and male BALB/c mice at ages 2, 4, 7, 12 and 20 months and evaluated their structural, densitometric and mechanical properties. MicroCT of the mid-diaphysis of the femur and radius indicated that during skeletal growth (2–7 months) bone cross-sectional size (area, moment of inertia) increased rapidly; during aging (7–20 months) cortical area was maintained while moment of inertia continued to increase. Bones from females were smaller than males at young ages, but not at later ages. Changes in whole-bone stiffness and strength reflected the changes in bone size, with a rapid increase from 2–7 months followed by little or no change. In contrast, energy-to-fracture declined with aging. Cortical tissue mineral density (TMD) increased during growth and was maintained with aging. MicroCT of trabecular bone revealed age-related changes that were site-dependent. The proximal tibia showed a clear pattern of age-related decline in trabecular BV/TV, with progressive decreases after 4 months in both sexes; lumbar (L5) vertebra had more modest age-related declines; in contrast, caudal (Ca7) vertebra had increasing BV/TV with aging. Overall, we found no evidence that females had more pronounced age-related deterioration than males. We conclude that bones from aging female and male BALB/c mice exhibit many of the changes seen in humans, and are therefore a clinically relevant model for studies of skeletal aging.

Keywords

bone structure; bone strength; bone mineralization; aging; mouse model

Introduction

With aging, there are deleterious changes in the structure and strength of the human skeleton. Some of these changes affect women more than men. For example, endosteal and periosteal expansion occurs in both women and men [1–5]. But at some sites the rate of endosteal expansion is greater in women [6], and at other sites periosteal expansion is not observed in women [4,7]. The net effect of these age-related changes in long bone morphology is that moment of inertia (a geometric measure of resistance to bending and torsion) may not increase in women as much as it does in men. At the material level, the strength of cortical bone declines with aging [8–11], with some evidence that this is worse in women [9]. Lastly, trabecular bone

Correspondence to: Matthew J. Silva, Department of Orthopaedic Surgery, Washington University School of Medicine, 11300 West Pavilion, 1 Barnes-Jewish Hospital Plaza, Saint Louis, MO 63110, 314-362-8585, silvam@wustl.edu.

DISCLOSURES: NONE

density and strength decrease dramatically from 20 to 80 years [12–13], leading to loss of bone strength at sites rich in trabecular bone [14–15]. Recent evidence suggests that declines in trabecular bone density after age 50 may be limited to women [16].

There are few descriptions of age-related changes in the structure and strength of mouse bones. Laboratory mice have an average lifespan of approximately 2 years [17], and mice aged 18–24 months are considered "old" [18]. Studies of mice in their first year of life indicate that bone structure develops rapidly from 0–2 months, while peak measures of bone mineral density (BMD) and cortical size are attained by 3–6 months [19–23]. There are few reports describing the skeletal changes that occur in the latter half of the mouse lifespan, especially with respect to mechanical properties. Glatt et al. [23] reported that trabecular bone volume peaks near 2 months in C57Bl/6 mice, followed by decreases throughout life that are more pronounced in females than males. Buie et al. [21] likewise reported an early peak in trabecular bone volume in female mice from three inbred strains (C57Bl/6, BALB/c, C3H/He), with evidence of decline after 6–8 months of age. Neither study examined mechanical properties. Ferguson et al. [22] reported that femoral periosteal size increases throughout life in male C57Bl/6 mice, yet stiffness and energy-to-fracture decrease after 1 year of age. There are no data on age-related changes in mechanical properties in female mice. In summary, although there is evidence of age-related skeletal deterioration in mice, analogous to changes in humans, additional data are needed to better describe age- and sex-dependent changes in bone structure and strength.

Our objective was to further evaluate the relevance of using mice for studies of age-related osteoporosis, with a focus on bone structure and strength. We evaluated structural, densitometric and mechanical properties of bones from female and male BALB/c mice aged 2 to 20 months.

Materials and Methods

Virgin female and male BALB/c mice were obtained at age 2, 4, 7, 12 and 20 months (102 total; n=8–11/group; National Institutes of Aging). With approval from our Animal Studies Committee, mice were euthanized upon arrival by CO_2 asphyxiation. We dissected femora, tibiae, radii, humeri, fifth lumbar (L5) and seventh caudal (Ca7) vertebrae (Table 1). Bones were wrapped in gauze soaked with phosphate buffered saline (PBS) and stored at −20°C until use.

Morphology, Density and Composition

The lengths of the right femora and radii were measured using calipers. These bones were then scanned by micro-computed tomography (CT) to assess diaphyseal morphology and density. CT slices transverse to the long axis were obtained along the central 3 mm of each diaphysis and results were averaged over these slices (Scanco μCT 40; 16 μm voxel size, medium resolution, 70 kV, 114 mA, 100 ms integration time). Tissue mineral density (TMD, calibrated to hydroxyapatite [HA]) of cortical bone was determined using the manufacturer's 3D analysis tools. Images were imported into ImageJ (NIH), rotated to align the x-axis with the subsequent bending axis, and binarized using a threshold midway between the median grayscale values for bone and background. From the coordinates of the bone pixels we computed bone area (B.Ar), bone moment of inertia ($B.I_{xx}$) and average cortical thickness (Ct.Th).

Left tibiae, L5 vertebrae and Ca7 vertebrae were scanned by microCT (as above) to assess trabecular bone morphology. For tibiae, total volume (TV) for analysis was a 480 μm (30 slice) region of the proximal metaphysis, distal to the growth plate, including all tissue inside the endosteal margin. The vertebral TV was the centrum of the vertebral body, from endplate to endplate and inside the endosteal margin. Using the manufacturer's 3D analysis tools (direct method), we determined volumetric bone mineral density (vBMD) of the TV, bone volume

fraction (BV/TV), trabecular thickness (Tb.Th), number (Tb.N) and separation (Tb.Sp). Age appropriate thresholds of 300 (2 mo), 340 (4 mo), and 355 (7–20 mo) were applied to segment bone from background. (Threshold values [0–1000 scale] were selected after analysis of scans from four L5 vertebra of each age. Scans were segmented manually to determine bone area. The average threshold that produced the best match to the manual values was determined.) The morphology and density of the left femoral neck was assessed based on transverse microCT scans of a 320 μm (20 slice) region at the center of the neck (21 μm voxel size, medium resolution, 70 kV, 57 μA, 300 ms integration time). A threshold of 330 was used for all samples. We determined total area (T.Ar), bone area (B.Ar), and vBMD of the total area.

Water, organic and ash contents of the right humeral diaphysis were determined gravimetrically as described [24]. After removal of marrow, bone wet weight, dry weight and ash weights were measured. Water content, organic content and ash content were computed.

Mechanical Testing

Load-to-failure tests were performed to evaluate whole-bone mechanical properties at sites comprised of cortical bone only (femoral and radial diaphyses) and at cortico-trabecular sites (L5 vertebra, femoral neck). Tests were conducted at room temperature on hydrated specimens using a materials testing machine (Instron 8841). Force (F) and displacement (d) data were collected at 60 Hz (Labview, National Instruments).

Left femora and radii were tested in three-point bending. Each bone was placed on two supports (span, L = 7 mm [femur] or 8 mm [radius]) and a transverse force was applied at the mid-diaphysis under displacement control (0.03 mm/s). Force-displacement data were converted to moment ($M = FL/4$) and normalized displacement ($d' = 12d/L^2$) and analyzed to determine rigidity, yield moment, ultimate moment, post-yield displacement and energy-to-fracture [24]. We then used beam theory equations to estimate material properties (modulus, yield stress, ultimate stress) for the radius, which is the long bone best suited for material property estimation due to its relatively high length:width ratio (~11:1) [25].

L5 vertebral bodies were tested in axial compression. Prior to testing, endplates were ground to remove cartilage and establish parallel transverse surfaces. As described [26], the lower (caudal) endplate was glued to a fixed aluminum platen using cyanoacrylate, while the upper (cephalad) endplate was contacted by a platen that displaced downward at 0.05 mm/s. Stiffness, yield and ultimate force were determined from force-displacement curves.

The necks of the right femora were tested by application of a transverse force at the femoral head intended to mimic physiological loading. The distal ends of the bones were embedded in PMMA to the level of the lesser trochanter and clamped so that the neck axis was oriented horizontally. A downward vertical force was applied on the femoral head at 0.1 mm/s. Stiffness, yield and ultimate force, post-yield displacement and fracture energy were determined from force-displacement curves.

Data Analysis

Two-way analysis of variance (ANOVA, Statview, SAS Institute) was used to determine the effects of age and sex on each outcome. Significance was defined as $p < 0.05$. If the two-way ANOVA indicated a significant age effect, but no sex effect or age-sex interaction, then post hoc analysis (Fisher's Protect Least Significant Differences test) of the two-way ANOVA was used to determine differences between each age (male and female pooled). If the two-way ANOVA indicated a significant age effect and either a sex effect or age-sex interaction, then one-way ANOVAs were used: a) to assess the effect of age on each sex separately, followed by post hoc testing if the age effect was significant; and b) to assess the effect of sex at each

age. Linear regression analysis was used to examine relationships between trabecular parameters. Results are presented as mean ± SD.

Results

Diaphyseal (Cortical) Morphology

Femoral and radial size at the mid-diaphysis increased with age. Bone area and moment of inertia reached peaks between age 7–20 months with no age-related decline (Fig. 1; Table 2). There was a significant age-sex interaction (by two-way ANOVA) for most diaphyseal measures, indicating that females and males aged somewhat differently. Generally, female bones were smaller than male bones at 2 and 4 months, but gained more size thereafter so that they were as large or larger than male bones at 20 months. For example, the moment of inertia of female bones increased progressively from 2 to 20 months, with total increases of 170% (femur) and 75% (radius). By contrast, the moment of inertia of the male femur increased by 60% from 2 to 20 months and the moment of inertia of the male radius did not increase with time ($p = 0.09$, one-way ANOVA). Cortical thickness also changed in a sex-dependent manner. In females, peak cortical thickness was attained at 12 months, followed by a small decrease from 12 to 20 months. In males, peak thickness was attained at 4 or 7 months and did not change thereafter.

Cortical Density and Composition

Cortical mineral density and ash fraction of increased progressively with age in both sexes, while water and organic contents decreased with age (Table 3). Tissue mineral density at the mid-diaphysis of the femur and radius increased by ~12% from 2 to 20 months, with the greatest changes from 2 to 4 months (Fig. 2). Ash fraction of the humerus increased by ~6% from 2 to 20 months. Water and organic contents were greatest at 2 or 4 months followed by a decline.

Diaphyseal (Cortical) Mechanical Properties

Consistent with changes in bone size, the bending stiffness (rigidity) and strength (yield and ultimate moments) of the femur and radius increased with age, reaching peaks at 7–20 months. During the 2–20 month interval, femoral stiffness and strength increased by ~100% in both females and males, while radial properties increased by ~50% (Fig. 3A, 3B; Table 4). The only evidence of an age-related decline was a modest (~15%) decrease from 12 to 20 months in yield and ultimate moment of the femur. Overall, stiffness and strength were lower in female bones compared to males (rigidity and yield moment, $p < 0.05$ by two-way ANOVA), although these differences were modest (< 20%). Female bones were less stiff than male bones at nearly all ages, while they were less strong than male bones at younger ages only (2–7 months).

Energy-to-fracture, which is viewed as a measure of overall fracture resistance, showed clear evidence of age-related decline in both femora and radii. The age for peak energy-to-fracture was not consistent, ranging from 2–12 months across groups (female, male) and bones (femur, radius). However, the lowest value for energy-to-fracture was always at 20 months, and was significantly lower by an average of 40% than the peak value (Fig. 3C, 3D; Table 4).

The estimated material strength of the radius varied with age (Fig. 4; Table 4) in a pattern similar to the age-related changes in TMD. Yield and ultimate stress increased by 13 and 9%, respectively, from 2 to 4 months ($p < 0.05$, post hoc test) but did not change after 4 months. Yield stress did not differ significantly between females and males, while ultimate stress was slightly greater in females ($p < 0.05$, two-way ANOVA).

Trabecular Morphology and Volumetric BMD

Trabecular morphology varied with age, but in a site-dependent manner. At the proximal tibia, bone volume fraction (BV/TV) was highest at 4 months and lowest at 20 months (Table 5; Fig. 5A). The age-related decline in BV/TV was comparable in females (−54% from 4 to 20 months) and males (−63%). At the L5 vertebra there was a strong age-sex interaction (Fig. 5B). In males, BV/TV varied with age in a similar pattern to the tibia, although the decline was less (−25% from 4 to 20 months). Females differed in that BV/TV did not peak until 12 months, followed by a 25% decline from 12 to 20 months. At the Ca7 vertebra, there was no evidence of an age-related decline in BV/TV in either sex (Fig. 5C). BV/TV increased progressively from 4 to 20 months. At all sites, age-related changes in vBMD matched those in BV/TV.

Trabecular morphology differed between males and females, also in a site-dependent manner. At the proximal tibia, BV/TV was greater in females overall ($p < 0.001$, two-way ANOVA), and in particular at 7 and 12 months ($p < 0.05$, post hoc test). Similarly at the L5 vertebra, BV/TV was greater in females than males overall ($p < 0.001$, two-way ANOVA) and in particular at 7, 12 and 20 months ($p < 0.05$, post hoc test). In contrast, at the Ca7 vertebra BV/TV was less in females than males overall ($p < 0.001$, two-way ANOVA) and in particular at 2 months ($p < 0.05$, post hoc test).

Age-related changes in trabecular BV/TV correlated with changes in trabecular number and thickness, although again there were differences at the three sites. Based on linear regression analysis, tibial BV/TV correlated strongly with trabecular number ($r^2 = 0.55$, $p < 0.001$) but weakly with trabecular thickness ($r^2 = 0.07$, $p < 0.01$). Similarly, BV/TV of the Ca7 vertebral correlated more strongly with trabecular number ($r^2 = 0.72$, $p < 0.001$) than trabecular thickness ($r^2 = 0.41$, $p < 0.001$). By contrast, at the L5 vertebra BV/TV depended weakly on trabecular number ($r^2 = 0.06$; $p = 0.016$) but strongly on trabecular thickness ($r^2 = 0.58$, $p < 0.001$).

Vertebral Mechanical Properties

The compressive properties of L5 vertebrae varied significantly with age and differed between sexes (Fig. 5D; Table 6). Stiffness, yield force and ultimate force in females reached peaks at 7–12 months and declined thereafter, while males peaked at 4–7 months and declined thereafter. For example, ultimate force declined by 23% in females from 12 to 20 months, while it declined in males by 44% from 7 to 20 months. Overall, females had superior properties to males, with greater stiffness and strength at 7–20 months. The variations in compressive properties with age and sex corresponded well with variations in trabecular BV/TV (Fig. 5B).

Femoral Neck Morphology and Mechanical Properties

The femoral neck at its midpoint was mainly comprised of a thick-walled ring of cortical bone, and its morphology varied significantly with age. In females, bone area and total area were least at the youngest age examined (2 months) and greatest at the oldest age (20 months), with an increase of 35% during this interval (Fig. 6A; Table 7). In males, the pattern was different, with peak values at 7 months followed by a decline of 15%. Because of this decline, males had significantly less bone area than females at 12 months ($p = 0.005$, post hoc test) and marginally less at 20 months ($p = 0.070$, post hoc test).

The mechanical properties of the femoral neck also varied with age, with some evidence of age-related decline. Ultimate force increased significantly from 2 to 7 months in both sexes (~25%), followed by a decline in males (−17% from 7 to 20 months) but not females (Table 7; Fig. 6B). Fracture energy was highest at 4 months, and declined ~50% in both females and males from 4 to 20 months (Fig. 6C).

Discussion

Our objective was to describe lifelong changes in skeletal structure, density and strength in female and male BALB/c mice. Analysis of the femur and radius indicates that cortical area and moment of inertia increase rapidly during growth (2–7 months) and then are maintained or continue to increase during aging (7–20 months). Cortical mineralization increases progressively throughout life. Whole-bone stiffness and strength generally reflect the changes in area and moment of inertia, with little or no age-related decrease. In contrast, energy-to-fracture declines with aging. Analysis of trabecular bone structure revealed age-related changes that were site-dependent. The proximal tibia exhibited an age-related decline in trabecular bone volume, with progressive decreases after 4 months of age. In contrast, Ca7 vertebra had increasing trabecular bone volume throughout life. Overall, bones from females were smaller than males at young ages, but there were no consistent differences between sexes at later ages. Importantly, we found no evidence that age-related deterioration was more pronounced in females than males.

The age-related changes in cortical morphology that we observed are similar to changes reported by others. Femoral cortical area in female and male C57Bl/6 mice increased rapidly in the first 4 months of life and was maintained thereafter [22–23,27]. Tibial area in male C57Bl/6 mice [28] and female C57Bl/6, C3H/He and BALB/c mice [21] increased rapidly in the first 6 months with no appreciable change after that. Similarly, we found that cortical area of the femur and radius in BALB/c mice increased rapidly up to 7 months, and then increased only slightly or was constant from 7 to 20 months. Moment of inertia (a geometric measure of resistance to bending and torsion that is strongly influenced by periosteal diameter) also increased rapidly from 2 to 7 months, and then continued to increase from 7 to 20 months (except for the male radius). This is consistent with the continued increase from 1 to 24 months in femoral total bone area and moment of inertia in male C57Bl/6 mice [22,28]. In summary, long bones from several inbred mouse strains exhibit rapid increases in cortical area in the first 6 months of life, followed by maintenance of cortical area with continued periosteal expansion with aging.

The cross-sectional geometry of the adult BALB/c femur is intermediate to other inbred mouse strains. Price et al [27] characterized femoral morphology in female A/J, C57Bl/6J and C3H/HeJ mice, and noted that femurs from each strain achieve function through a different combination of traits. Comparing their data at 6 months of age to our data from females at 7 months, bone area and cortical thickness of the BALB/c femur are greater than C57Bl/6 and A/J, but less than C3H. Polar moment of inertia of BALB/c (not shown) is greater than A/J, but less than C57Bl/6 and C3H. Therefore, BALB/c femurs are not at the extreme in any morphological trait and may be a good choice for studies where and intermediate phenotype is desired.

We observed age-related increases in mineralization consistent with most previous findings in mice [20–22,27]. For example, femoral ash fraction in male C57Bl/6 mice increased rapidly from 1 to 3 months and was maintained through 12 months [22]. Femoral ash fraction in female A/J, C57Bl/7 and C3H mice increased rapidly in the first 4 months of life but did not change from 4–12 months [27]. Tibial TMD in female C57Bl/6, C3H/He and BALB/c mice reached a plateau at approximately 5 months and did not decline through 12 months [21]. One study reported that femoral and humeral ash fraction in male C57Bl/6 mice decreased by ~5% from 12 to 24 months, which suggests that there is an age-related decline in mineralization [22]. In slight contrast, our data from several sites in BALB/c mice indicate that mineralization is maintained or slightly increased through 20 months of age, with no evidence of decline.

Results of our bending tests indicate that some long bone mechanical properties are maintained with aging while others decline, consistent with a previous report in C57Bl/6 mice. Femora from male C57Bl/6 mice attained peak bending stiffness and strength (ultimate force) at 12 months, with no decline through 24 months [22]. Our findings for the BALB/c femur and radius were similar, with peak values of stiffness and ultimate moment at 7–20 months followed by no decline (except a 20% decrease in ultimate moment of the female femur). These changes in whole-bone stiffness and strength are consistent with the patterns of increase in moment of inertia, mineralization and material properties. In contrast, fracture energy peaks earlier in life and then declines substantially. In C57Bl/6 males, femoral fracture energy peaked at 4 months and declined by more than 50% after 15 months [22]. In the current study, the age of peak fracture energy varied widely (2–12 months depending on sex and bone), but the lowest fracture energy was always observed at the oldest age we examined (20 months). This age-related decrease in fracture energy reflects the combined effects of changes in ultimate force (measure of strength) and post-yield displacement (measure of ductility). Consistent with a previous study [20], we found that post-yield displacement decreased sharply during growth, with further declines after 12 months. We attribute this decline to increased mineralization (noted above), as well as increased collagen crosslinks. Increased collagen crosslinks have been associated with loss of toughness in aging human bones [10], and in a previous study in mice we observed age-related increases in crosslinks [29]. In summary, while long-bone stiffness and strength are largely maintained with aging, fracture energy declines substantially due to a loss of ductility.

Age-related changes in trabecular morphology depended strongly on site. Our results at the proximal tibia are consistent with previous reports of age-related decreases in trabecular BV/TV at long bone metaphyses [21,23,28,30]. Trabecular BV/TV in the proximal tibia of male C57Bl/6 mice [28] and in the distal femur of female and male C57Bl/6 mice [23] decreased progressively from 2 to 24 months. In female BALB/c mice, trabecular BV/TV in the proximal tibia was stable from 4 to 11 months [21], consistent with our findings. A study in male BALB/c mice reported a 50% decrease in distal femur BV/TV from 4 to 24 months [30], similar to the 60% decrease we found at the proximal tibia from 4 to 20 months in males and females. At the lumbar spine the findings are less consistent. There are reports of decreased trabecular BV/TV in female and male C57Bl/6 mice starting at 2 months (L5) [23] and 7 months (L3) [21], but no changes in female BALB/c mice (L3) from 3 to 11 months [21]. We found *increases* in L5 trabecular BV/TV in females from 4 to 12 months, followed by decreases from 12 to 20 months. In males we found a modest decrease of 25% from 4 to 20 months. Lastly, in the Ca7 vertebra we previously reported no changes from 4 to 12 months in SAMR1 and SAMP6 mice [31]. Now we report *increasing* BV/TV from 4 to 20 months in BALB/c mice. In summary, trabecular BV/TV at the proximal tibia and distal femur in several mouse strains peaks at an early age (2–4 months) and then decreases with increasing age. In the spine peak values of BV/TV occur later, followed by modest bone loss in lumbar vertebrae but no bone loss in caudal vertebrae.

Most, but not all, of the age-related changes we observed in BALB/c mice mimic changes that occur in humans. First, our finding that cortical area is maintained while moment of inertia increases during aging is consistent with endosteal and periosteal expansion noted in human long bones [1–5]. Second, our finding of decreased trabecular BV/TV with aging at the proximal tibia and (to a lesser extent) the L5 vertebra corresponds with reports of trabecular bone loss at multiple sites in humans [12–13,15–16,32]. Notably, our finding of *increased* BV/TV with aging in caudal vertebra does not match this general pattern. Because the caudal vertebrae are non-weight bearing, they may respond differently than weight bearing bones to the same systemic factors. Regardless, our results suggest that the caudal vertebrae should be avoided in studies of skeletal aging. Third, we observed significant increases in cortical mineralization during growth followed by maintenance with aging, consistent with data from

human cortical bone [9,33]. Fourth, we found that that the strength of long bones was maintained with aging while fracture energy decreased. This result is consistent with studies of human cortical bone that found toughness declines more dramatically with aging than ultimate stress [8–11]. Fifth, we observed a decrease with aging in the compressive strength of lumbar vertebrae and in femoral neck fracture energy, consistent with human findings [14–15].

Comparing females and males, we found no consistent evidence that female bones had inferior structure or strength compared to males as aging progressed. This finding is in contrast to findings from humans [15–16]. We also found no evidence of greater variability within female groups. The female mice used in our study were group housed and not exposed to males, and thus it is likely that they did not have estrous cycles [34]. This would eliminate any possible effects of variations in sex hormones on the skeleton. However, it is unlikely that aged mice in these conditions can be considered a good model for post-menopausal women.

Our study had some other limitations. First, the oldest age we examined was 20 months, which is less than the median lifespan for BALB/c mice under laboratory conditions (25 months [17]). Mice aged 18–24 months are suitable for aging studies [18]. Accordingly, we detected many age-related changes from 12 to 20 months. In a study of male C57Bl/6 mice, age-related changes were evident by 18 months of age with few further changes from 18–24 months [22]. Thus, we conclude that mice 18 months or older can be considered “aged” in terms of skeletal characteristics. A second limitation is that our study was cross-sectional, and thus “age-related changes” were inferred from differences between age groups. There has been one longitudinal study in mice that focused on skeletal development rather than aging [21]. Although the use in vivo microCT enables longitudinal studies of bone structure, bone strength can not be measured in a longitudinal study.

In summary, we observed changes in bone structure and strength during growth and aging in BALB/c mice that mimic changes in humans. Diaphyseal sites exhibit periosteal expansion throughout life, while trabecular sites (proximal tibia and L5 vertebra) exhibit age-related bone loss. Cortical bone has increased mineralization during growth but little change with aging. Long bones maintain their stiffness and strength during aging, yet have decreased energy-to-fracture. Lastly, at the L5 vertebra and femoral neck, two sites prone to fracture in humans, bone strength and fracture energy are reduced with aging. We conclude that aging BALB/c mice have clinical relevance as a model of skeletal aging.

Acknowledgments

Supported by NIH/NIAMS grants R01AR047867 and P30AR057235 (Washington University Core Center for Musculoskeletal Biology and Medicine).

References

1. Ahlborg HG, Johnell O, Turner CH, Rannevik G, Karlsson MK. Bone loss and bone size after menopause. N Engl J Med 2003;349:327–334. [PubMed: 12878739]
2. Bouxsein ML, Myburgh KH, van der Meulen MC, Lindenberger E, Marcus R. Age-related differences in cross-sectional geometry of the forearm bones in healthy women. Calcif Tissue Int 1994;54:113–118. [PubMed: 8012866]
3. Martin RB, Atkinson PJ. Age and sex-related changes in the structure and strength of the human femoral shaft. J Biomech 1977;10:223–231. [PubMed: 858728]
4. Ruff CB, Hayes WC. Sex differences in age-related remodeling of the femur and tibia. J Orthop Res 1988;6:886–896. [PubMed: 3171769]

5. Szulc P, Seeman E, Duboeuf F, Sornay-Rendu E, Delmas PD. Bone fragility: failure of periosteal apposition to compensate for increased endocortical resorption in postmenopausal women. J Bone Miner Res 2006;21:1856–1863. [PubMed: 17002580]
6. Riggs BL, Melton LJ, Robb RA, Camp JJ, Atkinson EJ, Peterson JM, Rouleau PA, McCollough CH, Bouxsein ML, Khosla S. Population-based study of age and sex differences in bone volumetric density, size, geometry, and structure at different skeletal sites. J Bone Miner Res 2004;19:1945–1954. [PubMed: 15537436]
7. Martin B. Mathematical model for repair of fatigue damage and stress fracture in osteonal bone. J Orthop Res 1995;13:309–316. [PubMed: 7602391]
8. Burstein AH, Reilly DT, Martens M. Aging of bone tissue: mechanical properties. J Bone Jt Surg Am 1976;58:82–86.
9. McCalden RW, McGeough JA, Barker MB, Court-Brown CM. Age-related changes in the tensile properties of cortical bone. The relative importance of changes in porosity, mineralization, and microstructure. J Bone Jt Surg Am 1993;75:1193–1205.
10. Wang X, Shen X, Li X, Agrawal CM. Age-related changes in the collagen network and toughness of bone. Bone 2002;31:1–7. [PubMed: 12110404]
11. Zioupos P, Currey JD. Changes in the stiffness, strength, and toughness of human cortical bone with age. Bone 1998;22:57–66. [PubMed: 9437514]
12. McCalden RW, McGeough JA, Court-Brown CM. Age-related changes in the compressive strength of cancellous bone. The relative importance of changes in density and trabecular architecture. J Bone Joint Surg Am 1997;79:421–427. [PubMed: 9070533]
13. Mosekilde L, Mosekilde L, Danielson CC. Biomechanical competence of vertebral trabecular bone in relation to ash density and age in normal individuals. Bone 1987;8:79–85. [PubMed: 3593611]
14. Courtney AC, Wachtel EF, Myers ER, Hayes WC. Age-related reductions in the strength of the femur tested in a fall-loading configuration. J Bone Jt Surg Am 1995;77:387–395.
15. Ebbesen EN, Thomsen JS, Beck-Nielsen H, Nepper-Rasmussen HJ, Mosekilde L. Age- and gender-related differences in vertebral bone mass, density, and strength. J Bone Miner Res 1999;14:1394–1403. [PubMed: 10457272]
16. Lochmuller EM, Matsuura M, Bauer J, Hitzl W, Link TM, Muller R, Eckstein F. Site-specific deterioration of trabecular bone architecture in men and women with advancing age. J Bone Miner Res 2008;23:1964–1973. [PubMed: 18665791]
17. Harrison, DE. Baseline life span data: twelve strains of commonly used laboratory mice. 2009. http://research.jax.org/faculty/harrison/ger1vi_LifeStudy2.html
18. Flurkey, K.; Currer, JM.; Harrison, DE. Mouse models in aging research. In: Fox, JG.; Barthold, SW.; Davisson, MT., et al., editors. The mouse in biomedical research. 2nd edition. Vol. Vol. 3.. Academic Press; 2007. p. 637-672.
19. Beamer WG, Donahue LR, Rosen CJ, Baylink DJ. Genetic variability in adult bone density among inbred strains of mice. Bone 1996;18:397–403. [PubMed: 8739896]
20. Brodt MD, Ellis CB, Silva MJ. Growing C57Bl/6 mice increase whole bone mechanical properties by increasing geometric and material properties. J Bone Miner Res 1999;14:2159–2166. [PubMed: 10620076]
21. Buie HR, Moore CP, Boyd SK. Postpubertal architectural developmental patterns differ between the L3 vertebra and proximal tibia in three inbred strains of mice. J Bone Miner Res 2008;23:2048–2059. [PubMed: 18684086]
22. Ferguson VL, Ayers RA, Bateman TA, Simske SJ. Bone development and age-related bone loss in male C57BL/6J mice. Bone 2003;33:387–398. [PubMed: 13678781]
23. Glatt V, Canalis E, Stadmeyer L, Bouxsein ML. Age-related changes in trabecular architecture differ in female and male C57BL/6J mice. J Bone Miner Res 2007;22:1197–1207. [PubMed: 17488199]
24. Silva MJ, Brodt MB, Ettner SL. Long bones from the senescence accelerated mouse SAMP6 have increased size but reduced whole-bone strength and resistance to fracture. J Bone Miner Res 2002;17:1597–1603. [PubMed: 12211429]
25. Schriefer JL, Robling AG, Warden SJ, Fournier AJ, Mason JJ, Turner CH. A comparison of mechanical properties derived from multiple skeletal sites in mice. J Biomech 2005;38:467–475. [PubMed: 15652544]

26. Tommasini SM, Morgan TG, van der Meulen M, Jepsen KJ. Genetic variation in structure-function relationships for the inbred mouse lumbar vertebral body. J Bone Miner Res 2005;20:817–827. [PubMed: 15824855]
27. Price C, Herman BC, Lufkin T, Goldman HM, Jepsen KJ. Genetic variation in bone growth patterns defines adult mouse bone fragility. J Bone Miner Res 2005;20:1983–1991. [PubMed: 16234972]
28. Halloran BP, Ferguson VL, Simske SJ, Burghardt A, Venton LL, Majumdar S. Changes in bone structure and mass with advancing age in the male C57BL/6J mouse. J Bone Miner Res 2002;17:1044–1050. [PubMed: 12054159]
29. Silva MJ, Brodt MD, Wopenka B, Thomopoulos S, Williams D, Wassen MH, Ko M, Kusano N, Bank RA. Decreased collagen organization and content are associated with reduced strength of demineralized and intact bone in the SAMP6 mouse. J Bone Miner Res 2006;21:78–88. [PubMed: 16355276]
30. Bergman RJ, Gazit D, Kahn AJ, Gruber H, McDougall S, Hahn TJ. Age-related changes in osteogenic stem cells in mice. J Bone Miner Res 1996;11:568–577. [PubMed: 9157771]
31. Silva MJ, Brodt MD, Uthgenannt BA. Morphological and mechanical properties of vertebrae in the SAMP6 mouse model of senile osteoporosis. Bone 2004;35:425–431. [PubMed: 15268893]
32. Clarke BL, Ebeling PR, Jones JD, Wahner HW, O'Fallon WM, Riggs BL, Fitzpatrick LA. Changes in quantitative bone histomorphometry in aging healthy men. J Clin Endocrinol Metab 1996;81:2264–2270. [PubMed: 8964862]
33. Currey JD, Brear K, Zioupos P. The effects of ageing and changes in mineral content in degrading toughness of human femora. J. Biomech 1996;29:257–260. [PubMed: 8849821]
34. Whittingham, DG.; Wood, MJ. Reproductive physiology. In: Foster, HL.; Small, JD.; Fox, JG., editors. The mouse in biomedical research. 1st edition. Vol. Vol. 3.. Academic Press; 1983. p. 137-164.

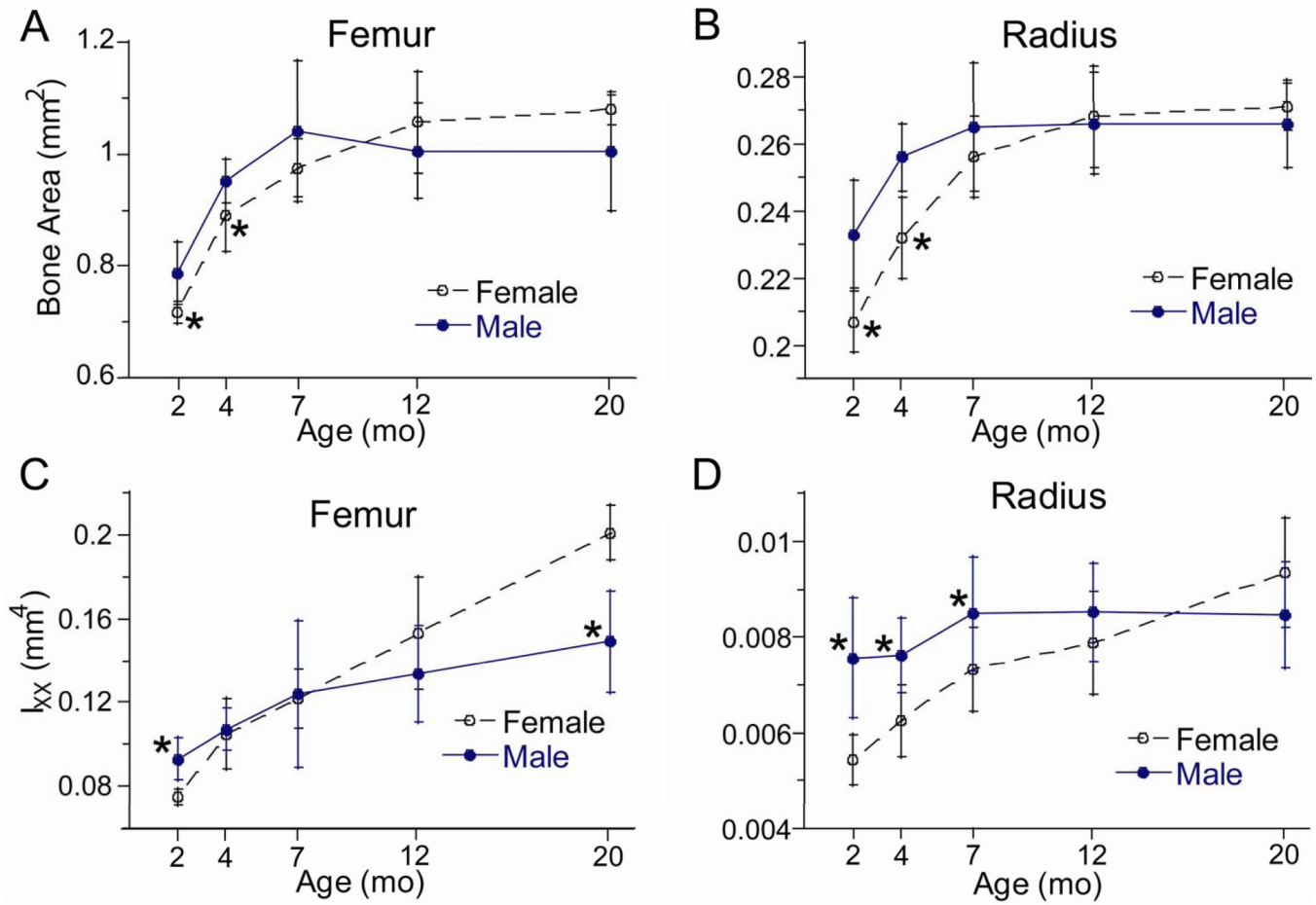

Figure 1.

Cross-sectional morphology of long bones from female and male BALB/c mice versus age. (A,B) Area and (C,D) moment of inertia were obtained from microCT scans at the mid-diaphysis of the femur and radius. (*female different from male at same age, $p < 0.05$)

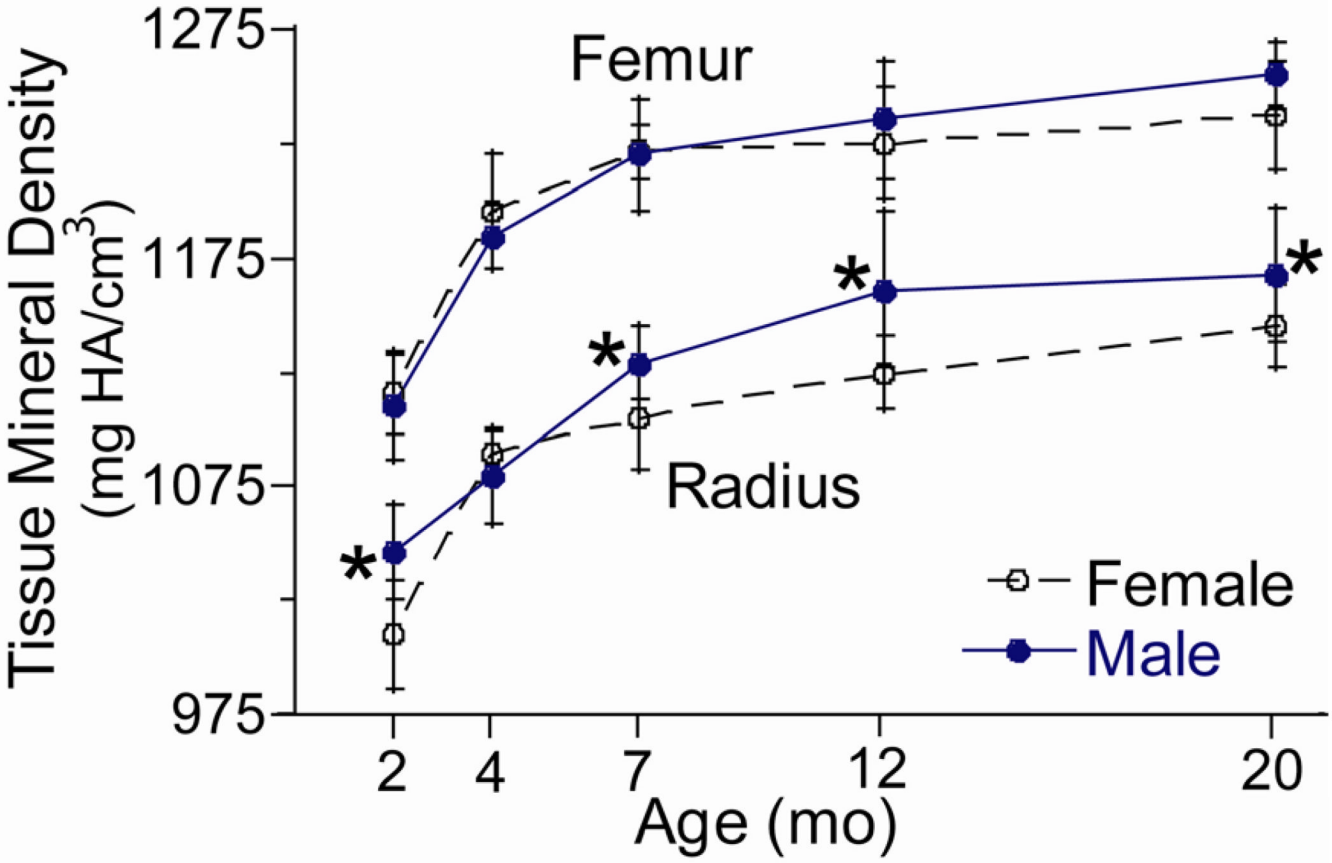

Figure 2.
Tissue mineral density (TMD) from female and male BALB/c mice versus age. TMD was determined from microCT at the mid-diaphysis.
(*female different from male at same age, $p < 0.05$)

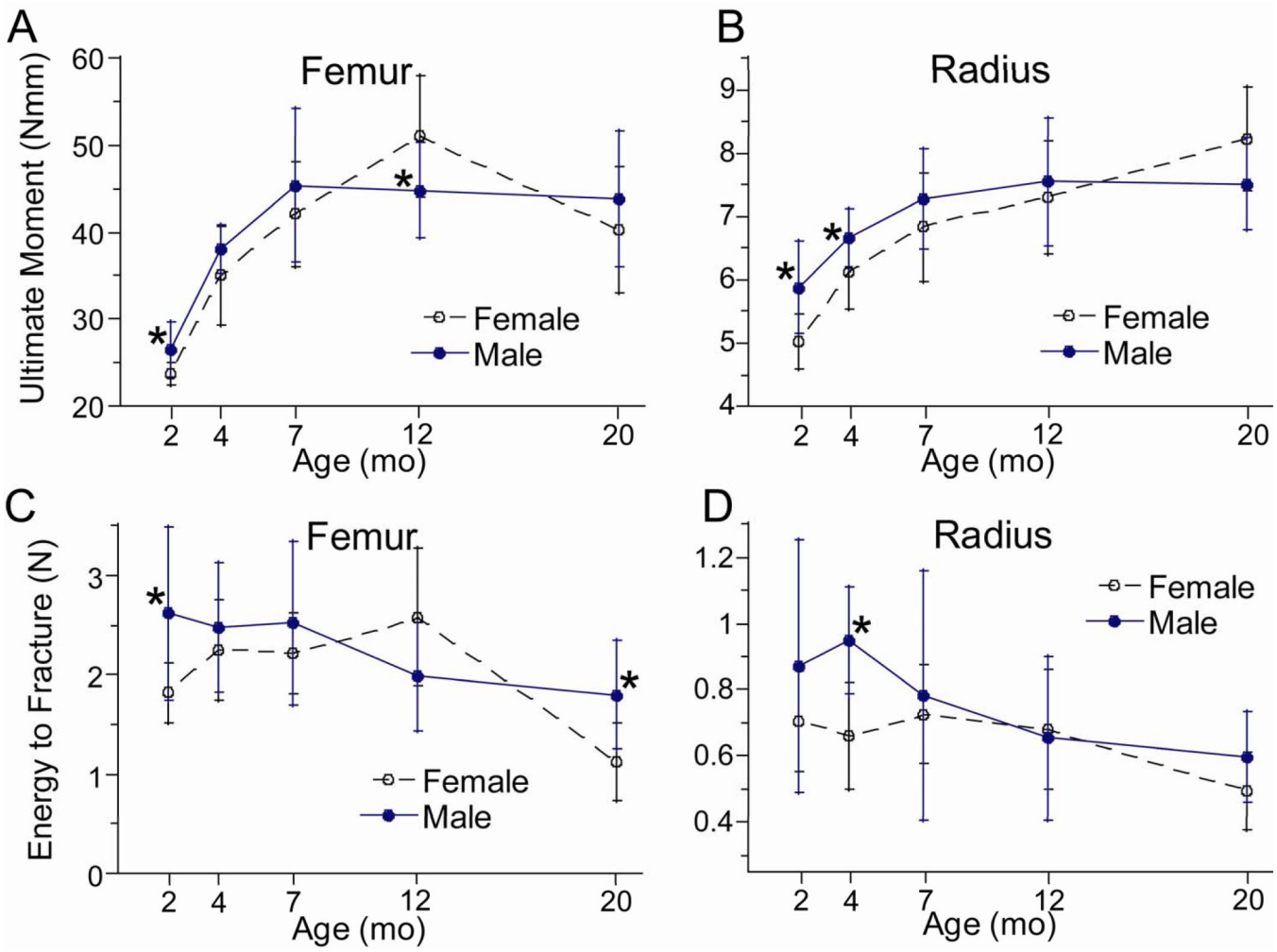

Figure 3.

Mechanical properties of long bones from female and male BALB/c mice versus age. (A,B) Ultimate moment (a measure of strength), and (C,D) energy-to-fracture (a measure of overall fracture resistance) were determined by three-point bending. (*female different from male at same age, $p < 0.05$)

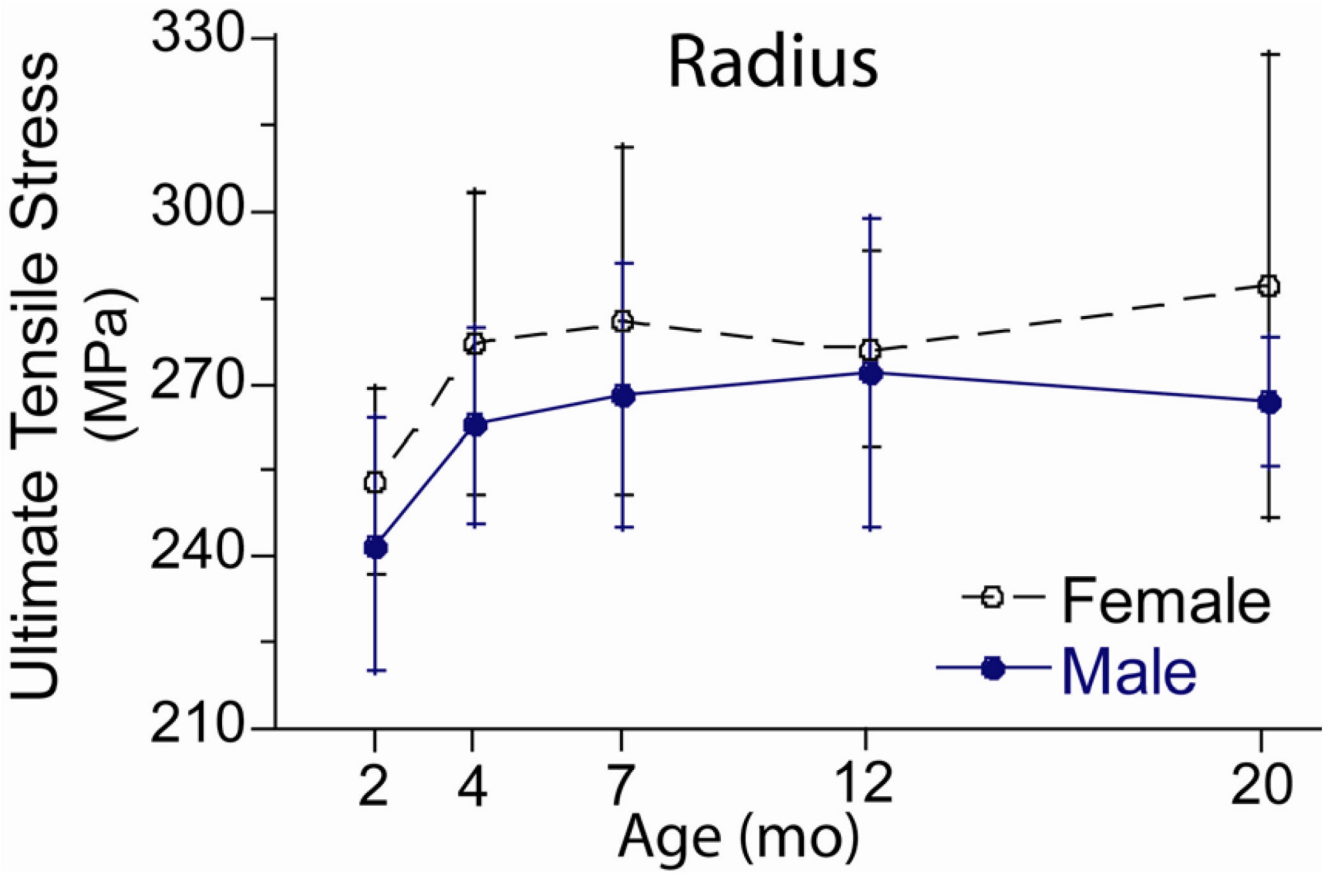

Figure 4.
Material strength of the radius from female and male BALB/c mice. Ultimate tensile stress was estimated from results of three-point bending tests and from cross-sectional geometry using beam theory.

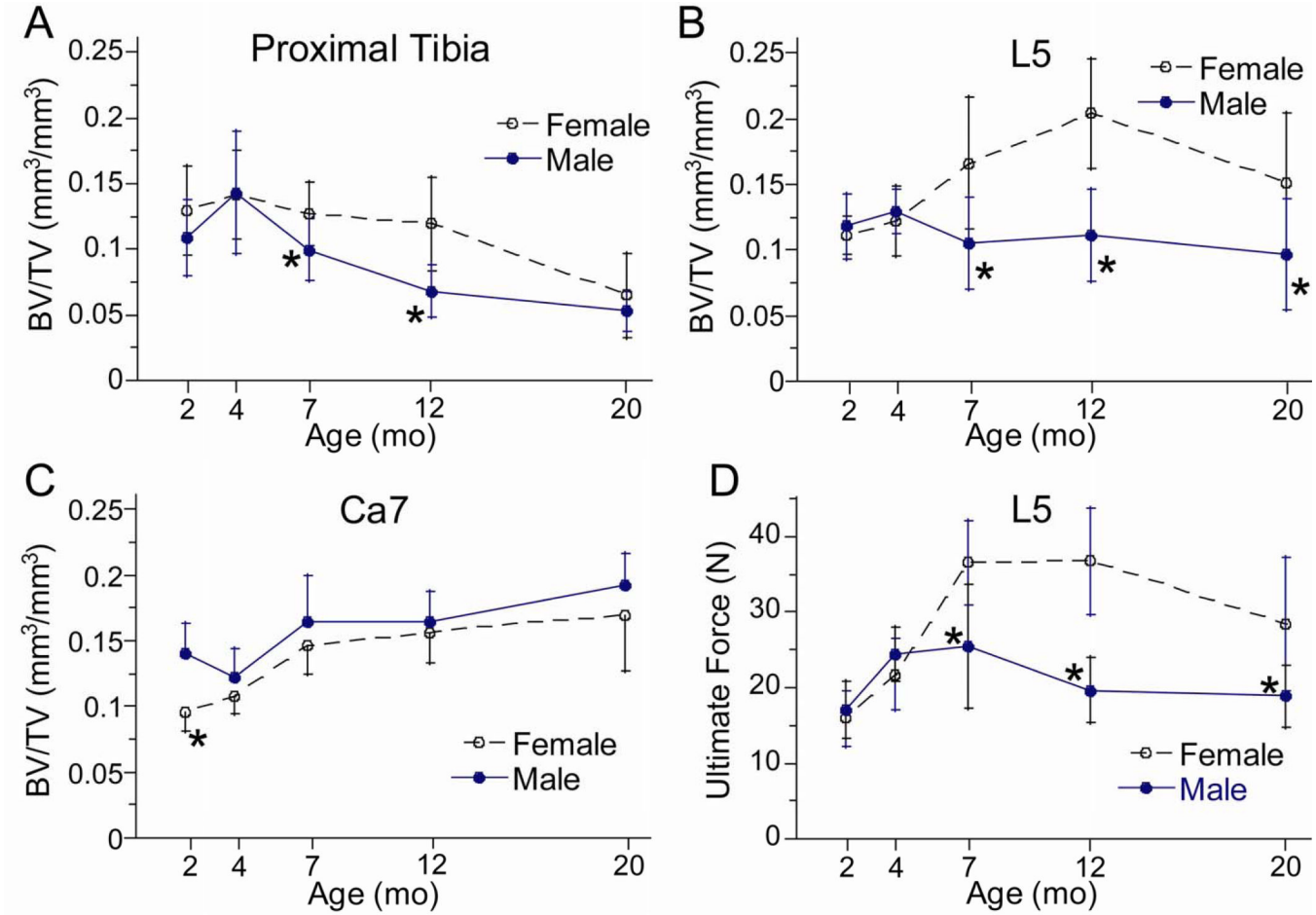

Figure 5.

Trabecular bone volume fraction (BV/TV) and L5 vertebral strength from female and male BALB/c mice versus age. Trabecular BV/TV was determined from microCT scans at the (A) proximal tibial metaphysis, (B) the 5th lumbar, and (C) the7th caudal vertebrae. (D) Ultimate force (a measure of strength) was determined by axial compression of the L5 vertebral body. (*female different from male at same age, $p < 0.05$)

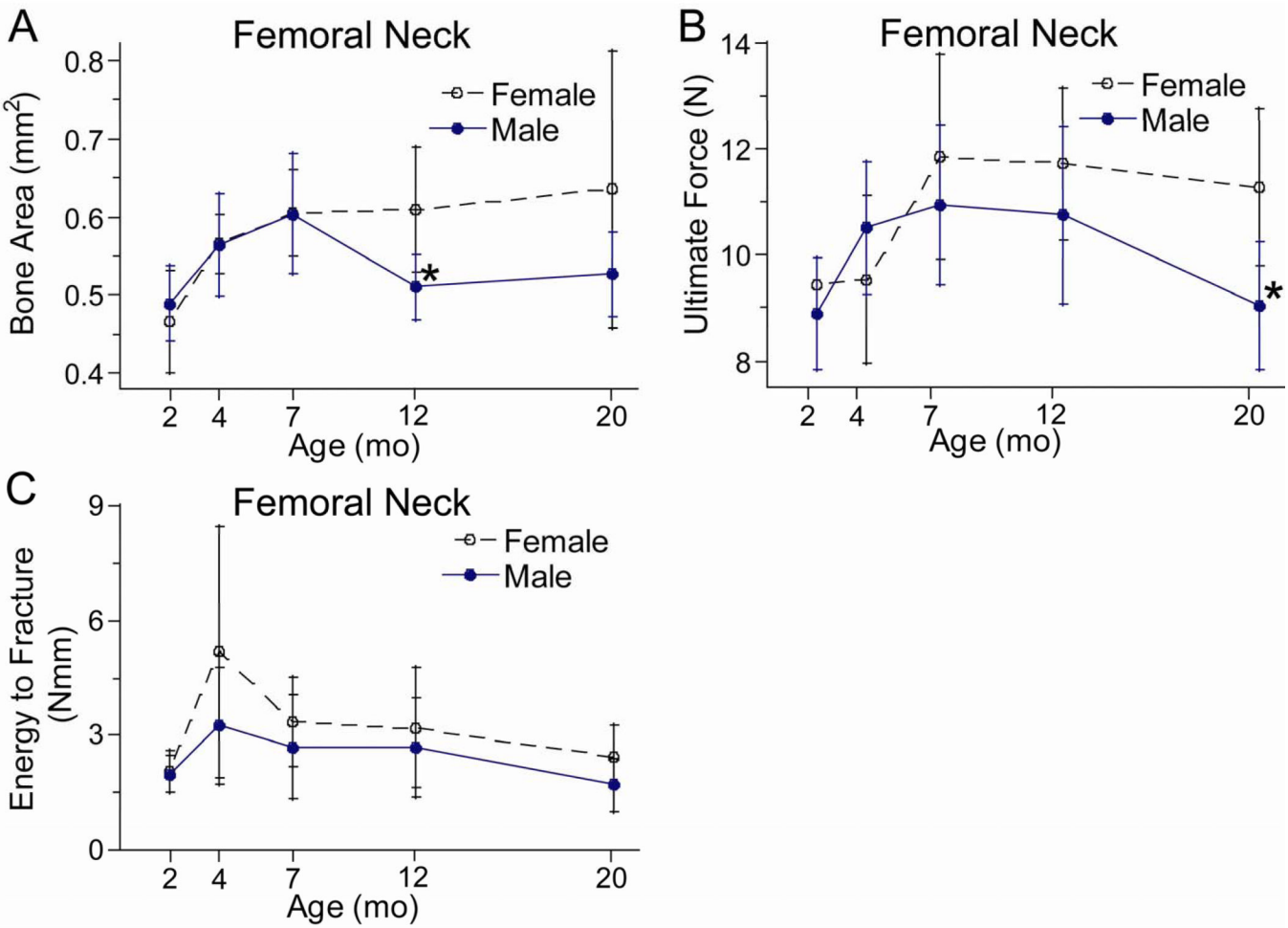

Figure 6.

Morphological and mechanical properties of the femoral neck from female and male BALB/c mice versus age. (A) Bone area was determined from microCT scans at the mid-neck. (B) Ultimate force (a measure of strength), and (C) energy-to-fracture (a measure of overall fracture resistance) were determined by a transverse loading of the femoral head. (*female different from male at same age, $p < 0.05$)

Table 1

List of bones and analysis techniques

Bone	Technique
Right Humerus	Gravimetric analysis (wet, dry, ash weight)
Left Femur	Femoral neck microCT
	Femoral neck mechanical testing
Right Femur	Diaphyseal microCT
	Diaphyseal three-point bending
Left Radius	Diaphyseal microCT
	Diaphyseal three-point bending
Left Tibia	Proximal metaphyseal microCT
5th Lumbar Vertebra (L5)	Vertebral body microCT
	Axial compression
7th Caudal Vertebra (Ca7)	Vertebral body microCT

Table 2

Body mass, and femoral and radial morphology

		Female					Male				
		2 mo. (n = 11)	**4 mo. (n = 10)**	**7 mo. (n = 10)**	**12 mo. (n = 10)**	**20 mo. (n = 8)**	**2 mo. (n = 11)**	**4 mo. (n = 10)**	**7 mo. (n = 10)**	**12 mo. (n = 10)**	**20 mo. (n = 10)**
Body Mass$^{A,S,A\text{-}S}$ (g)		19.4 ± 0.7	21.7^{a} ± 0.7	26.0^{a,b} ± 1.4	27.1^{a,b} ± 1.5	26.4^{a,b} ± 2.9	22.8* ± 1.1	26.3^{*,a} ± 1.1	31.9^{*,a,b} ± 4.5	30.5^{*,a,b} ± 2.7	26.0^{a,c,d} ± 5.2
Femur	Length^{A} (mm)	13.8 ± 0.4	15.3^{a} ± 0.3	15.9^{a,b} ± 0.2	16.2^{a,b} ± 0.4	16.5^{a,b,c,d} ± 0.3	13.9 ± 0.9	15.3^{a} ± 0.3	16.0^{a,b} ± 0.3	15.9^{a,b} ± 0.8	16.4^{a,b,c,d} ± 0.3
	Bone Area$^{A,A\text{-}S}$ (mm^2)	0.718 ± 0.019	0.891^{a} ± 0.065	0.975^{a,b} ± 0.052	1.057^{a,b,c} ± 0.091	1.079^{a,b,c} ± 0.026	0.786* ± 0.056	0.953^{*,a} ± 0.039	1.042^{a,b} ± 0.126	1.006^{a,b} ± 0.086	1.005^{a,b} ± 0.105
	Mom. Inertia$^{A,S,A\text{-}S}$ (mm^4)	0.075 ± 0.004	0.105^{a} ± 0.017	0.122^{a,b} ± 0.014	0.153^{a,b,c} ± 0.027	0.201^{a,b,c,d} ± 0.013	0.093* ± 0.010	0.107 ± 0.010	0.124^{a,b} ± 0.035	0.134^{a,b} ± 0.023	0.149^{*,a,b,c,d} ± 0.024
	Cortical Thickness^{A,S} (mm)	0.231 ± 0.015	0.271^{a} ± 0.016	0.285^{a} ± 0.013	0.301^{a,b} ± 0.025	0.275^{a,d} ± 0.016	0.257* ± 0.033	0.294^{*,a} ± 0.011	0.335^{*,a,b} ± 0.037	0.318^{a,b} ± 0.031	0.314^{*,a,b} ± 0.034
Radius	Length^{A,S} (mm)	10.4 ± 0.3	11.1^{a} ± 0.1	11.1^{a} ± 0.2	11.0^{a} ± 0.2	11.1^{a} ± 0.6	10.7 ± 0.4	11.2^{a} ± 0.2	11.7^{*,a,b} ± 0.4	11.6^{*,a,b} ± 0.3	11.5^{*,a} ± 0.4
	Bone Area$^{A,S,A\text{-}S}$ (mm^2)	0.207 ± 0.009	0.232^{a} ± 0.012	0.256^{a,b} ± 0.012	0.268^{a,b,c} ± 0.015	0.271^{a,b,c} ± 0.007	0.233* ± 0.016	0.256^{*,a} ± 0.010	0.265^{a} ± 0.019	0.266^{a} ± 0.015	0.266^{a} ± 0.013
	Mom. Inertia$^{A,S,A\text{-}S}$ (mm^4)	0.0054 ± 0.0005	0.0063^{a} ± 0.0007	0.0073^{a,b} ± 0.0009	0.0079^{a,b} ± 0.0011	0.0094^{a,b,c,d} ± 0.0013	0.0076* ± 0.0012	0.0076* ± 0.0008	0.0085* ± 0.0012	0.0085 ± 0.0010	0.0085 ± 0.0011
	Cortical Thickness$^{A,A\text{-}S}$ (mm)	0.147 ± 0.005	0.169^{a} ± 0.006	0.191^{a,b} ± 0.008	0.197^{a,b,c} ± 0.007	0.189^{a,b,d} ± 0.007	0.153* ± 0.007	0.180^{*,a} ± 0.006	0.183^{a} ± 0.008	0.183^{*,a} ± 0.007	0.179^{*,a} ± 0.009

Area, moment of inertia and thickness were determined at the mid-diaphysis using microCT

^{A}Significant effect of age;

^{S}Significant effect of sex;

$^{A\text{-}S}$Significant age-sex interaction; ANOVA, $p < 0.05$

*Male different from female at same age, $p < 0.05$ post hoc test

^{a}different from 2 mo;

^{b}different from 4 mo;

^{c}different from 7 mo;

^{d}different from 12 mo; $p < 0.05$ post hoc test

Table 3

Cortical mineral density of the femur and radius and composition of the humerus

	Female					Male				
	2 mo. (n = 10)	**4 mo. (n = 11)**	**7 mo. (n = 10)**	**12 mo. (n = 10)**	**20 mo. (n = 8)**	**2 mo. (n = 11)**	**4 mo. (n = 10)**	**7 mo. (n = 11)**	**12 mo. (n = 10)**	**20 mo. (n = 10)**
Femoral TMD^{A} (mg HA/cm^3)	1116 ± 18	1195^{a} ± 25	1122^{a,b} ± 11	1225^{a,b} ± 25	1238^{a,b,c,d} ± 23	1110 ± 24	1185^{a} ± 13	1220^{a,b} ± 23	1235^{a,b} ± 26	1256^{a,b,c,d} ± 14
Radial TMD$^{A,S,A\text{-}S}$ (mg HA/cm^3)	1010 ± 24	1090^{a} ± 9	1105^{a} ± 23	1125^{a,b,c} ± 16	1145^{a,b,c,d} ± 18	1046* ± 21	1080^{a} ± 21	1129^{*,a,b} ± 16	1161^{*,a,b,c} ± 34	1168* ^{a,b,c} ± 29
Water Content^{A,S} (g/g)	0.140 ± 0.025	0.146 ± 0.025	0.123^{a,b} ± 0.015	0.121^{a,b} ± 0.010	0.125^{b} ± 0.007	0.134 ± 0.016	0.119* ± 0.017	0.116 ± 0.023	0.110^{a} ± 0.016	0.116 ± .032
Organic^{A,S} (g/g)	0.241 ± 0.023	0.215^{a} ± 0.016	0.217^{a} ± 0.013	0.216^{a} ± 0.015	0.214^{a} ± 0.011	0.241 ± 0.019	0.234* ± 0.019	0.228 ± 0.023	0.224 ± 0.022	0.225 ± 0.023
Ash^{A} (g/g)	0.620 ± 0.015	0.640^{a} ± 0.011	0.660^{a,b} ± 0.015	0.662^{a,b} ± 0.013	0.661^{a,b} ± 0.010	0.626 ± 0.022	0.647^{a} ± 0.009	0.656^{a,b} ± 0.014	0.666^{a,b} ± 0.020	0.659^{a,b} ± 0.014

Cortical tissue mineral density (TMD) was determined at the mid-diaphysis by microCT, based on average density of the bone volume (BV); cortical composition was determined by gravimetric analysis of the humeral diaphysis

^{A}Significant effect of age;

^{S}Significant effect of sex;

$^{A\text{-}S}$Significant age-sex interaction; ANOVA, $p < 0.05$

*Male different from female at same age, $p < 0.05$ post hoc test

^{a}different from 2 mo;

^{b}different from 4 mo;

^{c}different from 7 mo;

^{d}different from 12 mo;

$p < 0.05$ post hoc test

Table 4

Mechanical properties of femoral and radial diaphysis

		Female					Male				
		2 mo. (n = 11)	**4 mo. (n = 10)**	**7 mo. (n = 10)**	**12 mo. (n = 10)**	**20 mo. (n = 8)**	**2 mo. (n = 11)**	**4 mo. (n = 10)**	**7 mo. (n = 10)**	**12 mo. (n = 9)**	**20 mo. (n = 10)**
Femur	Rigidity^{A,S} (Nmm^2)	557 ± 50	877^{a} ± 160	975^{a} ± 158	1184^{a,b,c} ± 155	1128^{a,b,c} ± 161	636* ± 90	906^{a} ± 93	1149^{*,a,b} ± 186	1202^{a,b} ± 271	1302^{*,a,b} ± 180
	Yield Moment^{A,S} (Nmm)	19.5 ± 1.4	26.2^{a} ± 1.7	30.1^{a,b} ± 4.3	33.7^{a,b,c} ± 4.6	28.9^{a,d} ± 4.6	21.3* ± 2.2	29.4^{*,a} ± 3.2	32.9^{a} ± 7.8	35.2^{a,b} ± 6.6	30.8^{a} ± 6.1
	Ultimate Moment$^{A,A\text{-}S}$ (Nmm)	23.7 ± 1.3	35.0^{a} ± 5.6	42.1^{a,b} ± 6.1	51.0^{a,b,c} ± 7.0	40.3^{a,d} ± 7.3	26.5* ± 3.1	38.0^{a} ± 2.8	45.4^{a,b} ± 8.9	44.8^{*,a,b} ± 5.5	43.9^{a,b} ± 7.8
	Post-Yield Displ.$^{A,A\text{-}S}$ (mm/mm^2)	0.065 ± 0.016	0.057^{a} ± 0.018	0.045^{a} ± 0.015	0.045^{a} ± 0.013	0.020 ^{a,b,c,d} 0.008	0.097* ± 0.046	0.054^{a} ± 0.016	0.047^{a} ± 0.014	0.033^{a} ± 0.012	0.036^{*,a} ± 0.016
	Energy-to-Fracture$^{A,S,A\text{-}S}$ (N)	1.82 ± 0.30	2.25 ± 0.50	2.22^{a} ± 0.41	2.58^{a,b} ± 0.69	1.13^{a,b,c,d} ± 0.39	2.62* ± 0.87	2.47 ± 0.65	2.52 ± 0.82	1.98^{a} ± 0.54	1.80 ^{*,a,c} ± 0.54
Radius	Rigidity^{A,S} (Nmm^2)	90 ± 8	122^{a} ± 17	126^{a} ± 19	137^{a} ± 17	150^{a,b,c} ± 23	120* ± 19	147^{*,a} ± 15	152^{*,a} ± 25	170^{*,a,b} ± 38	176^{*,a,b} ± 20
	Yield Moment^{A,S} (Nmm)	4.4 ± 0.4	5.4^{a} ± 0.6	5.7^{a} ± 0.7	6.2^{a,b} ± 0.8	6.9^{a,b,c,d} ± 0.9	5.0* ± 0.6	6.0^{*,a} ± 0.5	6.4^{*,a} ± 0.8	6.9^{a,b} ± 1.0	7.0^{a,b} ± 1.1
	Ultimate Moment$^{A,A\text{-}S}$ (Nmm)	5.0 ± 0.4	6.1^{a} ± 0.6	6.8^{a,b} ± 0.9	7.3^{a,b} ± 0.9	8.2^{a,b,c,d} ± 0.8	5.9* ± 0.7	6.7^{*,a} ± 0.5	7.3^{a} ± 0.8	7.6^{a,b} ± 1.0	7.5^{a,b} ± 0.7
	Post Yield Displ.^{A} (mm/mm^2)	0.192 ± 0.062	0.128 ± 0.048	0.104^{a,b} ± 0.036	0.086^{a,b} ± 0.036	0.044^{a,b} ± 0.016	0.191 ± 0.114	0.193* ± 0.050	0.119^{a,b} ± 0.090	0.096^{a,b} ± 0.067	0.091^{*,a,b} ± 0.052
	Energy-to-Fracture,^{A,S} (N)	0.71 ± 0.15	0.66 ± 0.16	0.73 ± 0.15	0.68 ± 0.18	0.50^{a,b,c,d} ± 0.12	0.87 ± 0.38	0.95* ± 0.16	0.78^{b} ± 0.38	0.66^{b} ± 0.25	0.60^{a,b} ± 0.14
Radius	Modulus,$^{A,,S,,A\text{-}S}$ (GPa)	16.5 ± 0.9	19.7^{a} ± 2.7	17.1^{b} ± 1.0	17.5^{b} ± 1.3	16.4^{b} ± 3.0	16.0 ± 1.9	19.3^{a} ± 1.7	18.0^{a} ± 2.1	19.9 ^{*,a} ± 3.3	20.9 ^{*,a,c} ± 2.3
	Yield Stress ^{A} (MPa)	221 ± 14	245^{a} ± 29	235^{a} ± 18	233^{a} ± 12	242^{a} ± 34	205* ± 17	238^{a} ± 15	235^{a} ± 25	248^{a} ± 32	249^{a} ± 19
	Ultimate Stress ^{A,S} (MPa)	253 ± 13	277^{a} ± 26	281^{a} ± 30	276 ± 17	287^{a} ± 40	242 ± 22	263^{a} ± 17	268^{a} ± 23	272^{a} ± 27	267^{a} ± 11

Mechanical properties were determined by three-point bending

^{A}Significant effect of age;

S Significant effect of sex;

A-*S* Significant age-sex interaction; ANOVA, $p < 0.05$

* Male different from female at same age, $p < 0.05$ post hoc test

a different from 2 mo;

b different from 4 mo;

c different from 7 mo;

d different from 12 mo;

$p < 0.05$ post hoc test

Table 5

Trabecular morphology and density of the proximal tibia, 5th lumbar and 7th caudal vertebrae

		Female					Male				
		2 mo. (n = 11)	**4 mo. (n = 10)**	**7 mo. (n = 10)**	**12 mo. (n = 10)**	**20 mo. (n = 8)**	**2 mo. (n = 11)**	**4 mo. (n = 10)**	**7 mo. (n = 10)**	**12 mo. (n = 10)**	**20 mo. (n = 10)**
Tibia	BV/TV^{A,S} (mm^3/mm^3)	0.130 ± 0.034	0.142 ± 0.034	0.127 ± 0.025	0.119 ± 0.036	0.065^{a,b,c,d} ± 0.032	0.109 ± 0.029	0.143^{a} ± 0.047	0.100^{*,b} ± 0.024	0.068^{*,a,b,c} ± 0.020	0.053^{a,b,c} ± 0.015
	Tb.Th$^{A,S,A\text{-}S}$ (mm)	0.045 ± 0.003	0.049^{a} ± 0.003	0.052^{a} ± 0.005	0.057^{a,b,c} ± 0.004	0.061^{a,b,c} ± 0.007	0.040* ± 0.002	0.053^{a} ± .015	0.047^{*,a} ± 0.002	0.046^{*,a} ± 0.004	0.045^{*,b} ± 0.003
	Tb.N^{A,S} (mm^{-1})	5.7 ± 0.4	5.2^{a} ± 0.6	4.7^{a,b} ± 0.4	4.2^{a,b,c} ± 0.2	3.8^{a,b,c,d} ± 0.4	6.0 ± 0.7	6.0^{*,a} ± 0.8	4.6^{a,b} ± 0.5	4.2^{a,b} ± 0.3	4.0^{a,b,c} ± 0.3
	Tb.Sp^{A,S} (mm)	0.184 ± 0.016	0.202^{a} ± 0.022	0.225^{a,b} ± 0.020	0.257^{a,b,c} ± 0.019	0.297^{a,b,c,d} ± 0.024	0.176 ± 0.028	0.178* ± 0.027	0.227^{a,b} ± 0.023	0.261^{a,b,c} ± 0.018	0.272^{*,a,b,c} ± 0.023
	vBMD$^{A,S,A\text{-}S}$ (mg HA/cm^3)	226 ± 24	266^{a} ± 32	268^{a} ± 28	246 ± 37	168^{a,b,c,d} ± 41	218 ± 21	271^{a} ± 27	231^{*,b} ± 39	183^{*,a,b,c} ± 26	152^{a,b,c,d} ± 26
L5 Vertebra	BV/TV$^{A,S,A\text{-}S}$ (mm^3/mm^3)	0.112 ± 0.015	0.122 ± 0.027	0.166^{a} ± 0.050	0.204^{a,b,c} ± 0.042	0.152^{a,d} ± 0.053	0.118 ± 0.025	0.130 ± 0.017	0.106* ± 0.035	0.111* ± 0.035	0.097^{*,a,b} ± 0.042
	Tb.Th$^{A,S,A\text{-}S}$ (mm)	0.047 ± 0.003	0.047 ± 0.002	0.057^{a,b} ± 0.006	0.058^{a,b} ± 0.005	0.056^{a,b} ± 0.004	0.042* ± 0.002	0.044* ± 0.002	0.043* ± 0.004	0.043* ± .005	0.041* ± 0.008
	Tb.N^{A,S} (mm^{-1})	3.6 ± 0.4	3.5 ± 0.4	3.4 ± 0.5	3.4 ± 0.4	2.5^{a,b,c,d} ± 0.5	4.3* ± 0.5	4.4* ± 0.3	3.9 ^{*,b} ± 0.6	3.9 ± 0.6	3.4^{*,a,b,c,d} ± 0.5
	Tb.Sp^{A,S} (mm)	0.289 ± 0.030	0.295 ± 0.032	0.331 ± 0.057	0.315 ± 0.044	0.423^{a,b,c,d} ± 0.092	0.238* ± 0.023	0.233* ± 0.016	0.270* ± 0.051	0.264* ± 0.041	0.323^{*,a,b,c,d} ± 0.079
	vBMD$^{A,S,A\text{-}S}$ (mg HA/cm^3)	209 ± 9	249 ^{a} ± 21	282^{a,b} ± 34	326^{a,b,c} ± 42	268^{a,d} ± 56	218 ± 32	269 ^{*,a} ± 12	253^{*,a} ± 39	253^{*,a} ± 29	206 ^{*,b,c,d} ± 59
Ca7 Vertebra	BV/TV^{A,S} (mm^3/mm^3)	0.096 ± 0.015	0.108 ± 0.014	0.147^{a,b} ± 0.022	0.156^{a,b} ± 0.023	0.170^{a,b,c} ± 0.043	0.140* ± 0.023	0.122 ± 0.022	0.164^{a,b} ± 0.036	0.164^{b} ± 0.024	0.192^{a,b,c,d} ± 0.025
	Tb.Th$^{A,S,A\text{-}S}$ (mm)	0.052 ± 0.003	0.052 ± 0.003	0.064^{a,b} ± 0.003	0.064^{a,b} ± 0.002	0.063^{a,b} ± 0.005	0.054 ± 0.002	0.049^{*,a} ± 0.002	0.058^{*,a,b} ± 0.002	0.057^{*,a,b} ± 0.002	0.061^{a,b,c,d} ± 0.001
	Tb.N^{A,S} (mm^{-1})	2.7 ± 0.3	2.7 ± 0.2	3.2^{a,b} ± 0.3	3.1 ^{a,b} ± 0.2	3.5^{a,b,c,d} ± 0.4	3.2* ± 0.3	3.0* ± 0.3	3.5^{b} ± 0.5	3.3 ± 0.4	3.5^{a,b} ± 0.4
	Tb.Sp^{A,S} (mm)	0.378 ± 0.040	0.385 ± 0.029	0.327^{a,b} ± 0.038	0.322^{a,b} ± 0.025	0.293^{a,b,c} ± 0.036	0.327* ± 0.033	0.347* ± 0.043	0.300^{b} ± 0.047	0.321 ± 0.046	0.290^{a,b} ± 0.033

		Female					Male				
		2 mo. (n = 11)	**4 mo. (n = 10)**	**7 mo. (n = 10)**	**12 mo. (n = 10)**	**20 mo. (n = 8)**	**2 mo. (n = 11)**	**4 mo. (n = 10)**	**7 mo. (n = 10)**	**12 mo. (n = 10)**	**20 mo. (n = 10)**
	vBMD^{A,S} (mg HA/cm^3)	139 ± 13	169^{a} ± 16	229^{a,b} ± 22	244^{a,b} ± 22	258^{a,b,c} ± 40	182* ± 24	204* ± 18	258^{a,b} ± 42	249^{a,b} ± 24	295^{*,a,b,c} ± 24

Morphology and volumetric BMD were determined by microCT; vBMD is based on density averaged over the tissue volume (TV)

^{A}Significant effect of age;

^{S}Significant effect of sex;

$^{A\text{-}S}$Significant age-sex interaction; ANOVA, $p < 0.05$

*Male different from female at same age, $p < 0.05$ post hoc test

^{a}different from 2 mo;

^{b}different from 4 mo;

^{c}different from 7 mo;

^{d}different from 12 mo;

$p < 0.05$ post hoc test

Table 6

Mechanical properties of L5 vertebrae

	Female					Male				
	2 mo. (n = 10)	**4 mo. (n = 11)**	**7 mo. (n = 9)**	**12 mo. (n = 9)**	**20 mo. (n = 7)**	**2 mo. (n = 11)**	**4 mo. (n = 10)**	**7 mo. (n = 10)**	**12 mo. (n = 9)**	**20 mo. (n = 8)**
Stiffness$^{A,S,A\text{-}S}$ (N/mm)	143 ± 74	244 ± 94	349^{a} ± 158	363^{a,b} ± 158	124^{d} ± 98	87* ± 35	283^{a} ± 60	219^{*,a} ± 98	123*, ^{b,c} ± 51	124*, ^{b,c} ± 98
Yield Force$^{A,S,A\text{-}S}$ (N)	13.8 ± 3.8	19.9^{a} ± 4.1	30.6^{a,b} ± 8.8	33.2^{a,b} ± 7.6	23.9^{a,d} ± 8.4	14.7 ± 3.9	21.8^{a} ± 4.1	23.2^{a} ± 9.1	15.5*, ^{b,c} ± 3.5	13.1*, ^{b,c} ± 6.3
Ultimate Force$^{A,S,A\text{-}S}$ (N)	15.9 ± 3.7	21.8^{a} ± 4.7	36.5^{a,b} ± 5.6	36.7^{a,b} ± 7.1	28.4^{a,b,c,d} ± 8.8	17.0 ± 3.8	24.4^{a} ± 3.6	25.4^{*,a} ± 8.2	19.7^{*,c} ± 4.3	18.9*, ^{b,c} ± 4.1

Mechanical properties were determined by axial compression of the vertebral body

^{A}Significant effect of age;

^{S}Significant effect of sex;

$^{A\text{-}S}$Significant age-sex interaction; ANOVA, $p < 0.05$

*Male different from female at same age, $p < 0.05$ post hoc test

^{a}different from 2 mo;

^{b}different from 4 mo;

^{c}different from 7 mo;

^{d}different from 12 mo;

$p < 0.05$ post hoc test

Table 7

Femoral neck morphology, density and mechanical properties

	Female					Male				
	2 mo. (n = 11)	**4 mo. (n = 11)**	**7 mo. (n = 10)**	**12 mo. (n = 10)**	**20 mo. (n = 8)**	**2 mo. (n = 11)**	**4 mo. (n = 10)**	**7 mo. (n = 11)**	**12 mo. (n = 9)**	**20 mo. (n = 11)**
Bone Area$^{A,S,A\text{-}S}$ (mm^2)	0.466 ± 0.065	0.566^{a} ± 0.038	0.606^{a} ± 0.055	0.609^{a} ± 0.080	0.635^{a} ± 0.177	0.489 ± 0.048	0.564^{a} ± 0.065	0.604^{a} ± 0.076	0.511^{*,c} ± 0.042	0.527^{c} ± 0.054
Total Area^{A} (mm^2)	0.546 ± 0.051	0.607 ± 0.051	0.657^{a} ± 0.078	0.640 ± 0.088	0.739^{a,b} ± 0.240	0.619 ± 0.066	0.641 ± 0.094	0.718^{a,b} ± 0.096	0.615^{c} ± 0.064	0.690^{a,d} ± 0.059
TMD^{A,S} (mg HA/cm^3)	1111 ± 38	1236^{a} ± 32	1234^{a} ± 31	1262^{a} ± 22	1235^{a} ± 64	1073* ± 34	1194^{*,a} ± 11	1196^{*,a} ± 30	1220^{*,a} ± 33	1221^{a,b,c} ± 31
Stiffness (N/mm)	28.9 ± 6.6	17.8 ± 7.9	30.8 ± 14.7	28.9 ± 9.7	31.2 ± 13.0	24.1 ± 7.7	27.7 ± 9.3	33.2 ± 11.5	28.9 ± 9.7	32.0 ± 7.1
Yield Force$^{A,A\text{-}S}$ (N)	8.2 ± 0.58	6.5 ± 2.22	10.7^{a,b} ± 1.99	10.8^{a,b} ± 1.42	9.9^{b} ± 2.40	8.1 ± 0.78	8.8 ± 2.58	9.4 ± 2.04	9.5 ± 1.90	7.6^{*,c,d} ± 2.14
Ultimate Force$^{A,S,A\text{-}S}$ (N)	9.4 ± 0.51	9.5 ± 1.59	11.9^{a,b} ± 1.94	11.7^{a,b} ± 1.43	11.3^{a,b} ± 1.47	8.9 ± 1.07	10.5^{a} ± 1.25	10.9^{a} ± 1.52	10.9^{a} ± 1.69	9.0^{*,b,c,d} ± 1.20
Post-Yield Displ.^{A} (mm)	0.093 ± .0.48	0.417^{a} ± 0.394	0.092^{b} ± 0.101	0.190^{b} ± 0.450	0.055^{b} ± 0.089	0.051 ± 0.098	0.344^{a} ± 0.600	0.120^{b} ± 0.135	0.103^{b} ± 0.112	0.093^{b} ± 0.145
Energy-to-fracture^{A,S} (Nmm)	2.05 ± 0.55	5.18^{a} ± 3.30	3.37 ± 1.17	3.20 ± 1.58	2.45^{b} ± 0.81	1.98 ± 0.48	3.25^{a} ± 1.53	2.70 ± 1.36	2.68 ± 1.29	1.71^{b,c} ± 0.69

Morphology and tissue mineral density (TMD) determined by microCT at the center of the femoral neck; TMD is based on average density of the bone volume (BV); mechanical properties determined by transverse loading applied to femoral head

^{A}Significant effect of age;

^{S}Significant effect of sex;

$^{A\text{-}S}$Significant age-sex interaction; ANOVA, $p < 0.05$

*Male different from female at same age, $p < 0.05$ post hoc test

^{a}different from 2 mo;

^{b}different from 4 mo;

^{c}different from 7 mo;

^{d}different from 12 mo;

$p < 0.05$ post hoc test